Anomaly of the rotational non-ergodicity parameter of glass formers probed by high field electron paramagnetic resonance

V.Bercu,[1,2,3] M.Martinelli,[2] C.A. Massa,[2] L.A Pardi,[2] E.A.Rössler,[4] and D.Leporini[1,5,*]

[1]*Dipartimento di Fisica "Enrico Fermi", Università di Pisa, Largo B. Pontecorvo 3, I-56127 Pisa, Italy*

[2]*IPCF-CNR, via G.Moruzzi 1, I-56124 Pisa, Italy*

[3]*Department of Physics, University of Bucharest, Magurele, RO-76900, Bucharest, Romania*

[4]*Experimentalphysik II, Universität Bayreuth Universitätsstraße 30, D-95440 Bayreuth, Germany*

[5]*SOFT-INFM-CNR, Largo B. Pontecorvo 3, I-56127 Pisa, Italy*

(Dated: July 31, 2008)

Abstract

Exploiting the high angular resolution of high field electron paramagnetic resonance measured at 95, 190, and 285 GHz we determine model independently the rotational non-ergodicity parameter of different probe molecules in the glass former o-terphenyl and polybutadiene. Our results clearly show a characteristic change in the temperature of the non-ergodicity parameter proving a rather sharp dynamic crossover in both systems, in contrast to previous results from other techniques.

PACS numbers: 64.70.P-,64.70.Q-,76.30.-v

The problem - The most advanced description of the glass transition phenomenon is provided by the mode coupling theory (MCT) which emphasizes the role of the cage in which the molecules are caught for a finite time due to packing constraints [1, 2]. **The ideal MCT (IMCT) predicts** the existence of a sharp dynamic crossover, *i.e.*, a transition from liquid-like to solid-like dynamics, at a critical temperature, T_c **leading to characteristic scaling laws for density correlations and, particularly, a cusp-like anomaly in the temperature dependence of the non-ergodicity parameter f_q.** The latter represents the height of the intermediate plateau of the two-step density correlation decay, i.e. from an experimental view the relaxation strength of the structural relaxation or α-process. Apart from a few *model-dependent* experimental outcomes [1, 3–5], most studies concluded that the transition **, and then the anomaly of f_q,** is smeared out [1, 2]. **In particular,** a re-evaluation of early neutron scattering (NS) results even ended with the statement that there is "no sign of any critical singularity above the glass transition temperature" [6]. From the avoidance of the IMCT transition the role of phonon assisted "hopping processes" becoming relevant at low temperatures was stressed [1, 2, 7, 8]. In systems like colloids where phonons are not existing the structural arrest is well accounted for by IMCT [2, 9]. Thus, one may argue that the sharp transition is masked by additional ergodicity restoring processes typical of molecular systems. However, as it turns out to be difficult to identify the transition, one could also say there lies a major problem of the theory. **The missing evidence of the anomaly of the non-ergodicity parameter motivated the search of other signatures of the IMCT singularity. From this respect, verification of IMCT scaling properties [10], consistent fits of experimental data by using two-correlators versions [11, 12] and numerical assessment of IMCT predictions on vibrational excitations [13] and transport properties [14] were reported. Nonetheless, IMCT scaling fails in pressure/temperature studies of o-terphenyl (OTP) [15].**

This Communication reports on identifying the rotational analogue f_{rot} of the non-ergodicity parameter by using suitable paramagnetic probe molecules (spin probes) which couple to the glassy dynamics of the host [16–19]. **Use of probe molecules in glassformers and polymers is well documented also for other spectroscopies, like NMR [20], dielectric relaxation [21] and light spectroscopies [22].** We note that indications of the anomaly in $f_{rot}(T)$ were identified by light scattering experiments but again the transition was not sharp and the analysis relied on certain assumption which can be

challenged [5]. Generally, the problem is to correctly separate the contribution from fast and slow dynamics. In the present contribution, model-independent evidence is presented that the reorientation of probe molecules undergoes a sharp transition when dissolved in the glassformer OTP and in polybutadiene (PB). The crossover temperatures T_c agree with the less marked signatures obtained by previous experiments, and the present results become only possible by exploiting the extraordinary angular resolution of high field EPR.

The method - Usually, in glass forming systems one assumes high coupling between density fluctuations and rotational dynamics, and a similar scenario as in the case of the density correlation function is expected [23]. Explicitly, close to T_c IMCT predicts that the rotational correlation functions drops at intermediate times at a plateau $f_{rot}(T)$, the rotational non-ergodicity parameter, which originates from a *highly hindered* reorientation within the cage, whereas at long times it finally decays due to the isotropization driven by the α-process. $f_{rot}(T)$ is expected to show the typical signature of a cusp-like behavior at T_c:

$$f_{rot}(T) = f_{rot}^c + \begin{cases} h_{rot}\sqrt{T_c - T}, & T \leq T_c \\ \text{const}, & T > T_c \end{cases} \tag{1}$$

Our study was carried out by observing the influence of the reorientation of suitable spin probes dissolved in glass formers on the lineshape of high-field electron paramagnetic resonance (HF-EPR) [24, 25]. The EPR line shape of the spin probe is determined by the anisotropy of the g-tensor and the hyperfine interactions. When the molecules rotate, the couplings become time dependent which modifies the EPR lineshape provided that motion occurs in the EPR time window [24]. During the last years, HF-EPR techniques were developed to detect resonances under large magnetic fields by using electromagnetic radiation close to the far-infrared region (Larmor frequency $\nu_L \sim 0.1 - 0.6THz$), i.e., at much higher Larmor frequencies than conventional EPR ($\nu_L \sim 10GHz$) [25]. One major benefit is the remarkably enhanced orientation resolution.

In a magnetic resonance experiment (EPR as well as NMR), if the tagged species is frozen (no reorientation), the lineshape has a characteristic rigid solid (powder) pattern with width δ reflecting the characteristics coupling of the spins, in EPR the particular g-tensor and hyperfine interaction [24, 25]. Heating above T_g structural relaxation sets in involving first of all an un-hindered reorientation of the tagged species with correlation time τ_α. Initially the lineshape keeps the solid-like appearance. This slow motion regime is characterized by

the condition $\tau_\alpha\delta \gg 1$. For $\tau_\alpha\delta > 1$ a smooth broadening may be observed, *i.e.* the apparent width δ_{app} gets a bit smaller. The extent of this broadening and the temperature interval of its observation depends somewhat on the molecular mechanism involved, *e.g.*, large angle vs. small angle jumps, cf. below. Passing through the condition $\tau_\alpha\delta \sim 1$ the lineshape completely collapses, and for $\tau_\alpha\delta \ll 1$ the EPR interactions are averaged out by the fast isotropic reorientation of the probe molecule and only a spectrum of the isotropic hyperfine interaction is observed. Such a behavior is observed for the spin probe ANDRO dissolved in OTP, see Fig. 1(top).

As discussed, in addition to the α-process, a fast process exists in glass formers which is well documented by experiments and is attributed to highly hindered reorientations within the cage. This fast dynamics occurs in the ps range and its time scale τ_{fast} virtually does not change with temperature but only its amplitude and therefore its relaxation strength $(1 - f_{rot})$ [1, 5]. Thus, we assume that for this additional motion the condition $\tau_{fast}\delta \ll 1$ is fulfilled. The effect of this fast motion leads to a reduced pre-averaged coupling constant $\overline{\delta} \lesssim \delta$, where $\overline{\delta} = \delta R_{rot}$ with a reduction factor R_{rot}. As in the case of NMR [26], the reduction factor R_{rot} is related to the plateau value of the reorientational correlation function via $f_{rot} = R_{rot}^2$. Therefore, the temperature dependence of $\overline{\delta}$ tracks the one of the rotational non-ergodicity factor $f_{rot}^{1/2}$ and, according to IMCT, is expected to reflect the cusp-like behaviour of eq. 1.

The pre-averaging effect of the fast reorientation is only experimentally accessible provided that the pre-average $\overline{\delta} \lesssim \delta$ is detected well inside the slow motion regime, i.e. $\tau_\alpha\delta \gg 1$, where the α-process essentially does not affect the solid-state spectrum. In order that the condition $\tau_\alpha\delta \gg 1$ is fulfilled up to temperatures as high as possible, δ should be as large as possible. For example, with solid-state ^{2}H NMR one can not explore high temperatures in the viscous liquid; the NMR solid-state spectrum ($\delta/2\pi \simeq 100kHz$) collapses before T_c is reached. In contrast, high field EPR can easily reach $\delta/2\pi \simeq 1GHz$, and this we exploited in the present study.

Experiments and discussion - The glassformer OTP, and PB (M_w= 200 kg mol^{-1}, polydispersity 1.64) and the spin probes (with electron and nuclear spin $S = 1/2$ and $I = 1$, respectively) were obtained from Aldrich and used as received. **The spin probes will be referred to as: ANDRO (17β-Hydroxy-4',4'-dimethylspiro(5α-androstane-3,2'-oxazolidin)-3'-yloxy), NONA (10-Doxyl-nonadecane: 4,4-dimethyl-2,2-**

di-nonyloxazolidin-3-yloxyl), TEMPO (2,2,6,6-Tetramethyl-1-piperidinyloxy). The structures of both the glassformers and the spin probes are sketched in Figs. 3, 4. The spin probes were less then 0.08% in weight leading to undetectable mutual interactions among the probe molecules and no plasticization of the hosts. The EPR experiments were carried out on a home-built, ultrawide-band continuous-wave EPR spectrometer at $\nu_L = 95, 190$ and $285GHz$ [27] and profited by previous studies on both OTP and polymers by using conventional X-band low-field EPR [16, 17].

Figure 1(top) illustrates the temperature dependence of the EPR lineshape of ANDRO in OTP recorded at $\nu_L = 285$ GHz (note that the spectra are in the derivative mode). At temperatures below $T_g = 243K$ the pattern of the lineshape hardly changes. This is the rigid solid limit, *i.e.*, the isotropic reorientation of the spin probe is absent and cannot affect the lineshape. On heating above T_g, initially the lineshape still keeps the solid-like appearance, the only effect being a minor shrinking of the overall width accompanied by some slight broadening. Here the slow motion limit applies as $\tau_\alpha \delta \gg 1$, $\delta \sim 2\pi 1.4$ GHz at $\nu_L = 285$ GHz holds. As temperature increases above $\sim 313K$ the lineshape starts to collapse, that is the EPR frequencies are effectively averaged by the now fast isotropic reorientation attributed to the α-process of the host. At ~ 338 K the complete collapse has essentially taken place owing to rapid reorientation with correlation time $\tau_\alpha \sim \delta^{-1} \sim 0.1$ ns. For a first comparison we included in Fig. 1(top) the time τ_α of OTP as found in ref. [4] **(p.1484)**. Clearly τ_α at $T \lesssim 300K$ is too long to significantly affect the EPR lineshape ($\delta\tau_\alpha \gtrsim 70$). In contrast, above 313 K the time constants τ_α are short enough achieving a complete collapse of the solid-state spectrum within a very narrow temperature interval.

Figure 1(bottom) plots a series of graphically superimposed spectra obtained in the temperature range $292.1K \leq T \leq 307.3K$. Increasing the temperature up to 297.8 K affects the spectra with well recognized broadening and shifts of the spectral features (singularities). However, in the range $297.8K \leq T \leq 304.5K$ no spectral changes are observed at all; the lineshapes (full lines in Fig.1, bottom) superimpose perfectly. Only at 307.3 K a further change towards the full collapse of the line is observed. Notice that in the range $297.8K \leq T \leq 304.5K$ τ_α changes by a factor of three, however, virtually no change is found in the spectra in that temperature range.

In order to study the spectral changes *in a model-independent way*, we considered the temperature dependence of the spectral spacing ΔB_{ν_L} between well selected singularities of

the EPR spectrum at the Larmor frequency ν_L [18]. ΔB_{ν_L} yields a measure of the overall width δ_{app} which as a start we distinguish from $\overline{\delta}$. The chosen spacing ΔB_{ν_L} was varied according to the different Larmor frequencies applied. Fig. 2 shows the low-temperature EPR spectra at two Larmor frequencies ν_L ($\nu_L = 95, 285 GHz$), and specifies the choice of the spacing ΔB_{ν_L} [28].

Figure 3 reports the temperature dependence of the spectral parameter ΔB_{ν_L} for $\nu_L = 95, 190$ and $285 GHz$. The trends observed as a function of temperature are very similar and reproduce the qualitative observation made above; four regimes can be identified. Starting at low temperatures only a minor change of ΔB_{ν_L} is observed (regime I), approaching 280 K a much stronger decrease with temperature sets in which for all frequencies stops at 297.5 ± 0.5 K (regime II). Above that temperature a plateau-like feature in ΔB_{ν_L} vs T is observed (regime III). We reiterate that in regime II as well as in regime III still the essential features of a solid-state spectrum are observed. At the highest temperatures, again a strong decrease is observed (regime IV), reflecting the onset of the collapse of the lineshape due to the α-process. Owing to the linear increase of the overall width of the lineshape with the Larmor frequency (g-tensor interaction is proportional to the Larmor frequency), the onset of the influence of the α-process is expected to shift to higher temperature. Consequently, the width of the plateau is largest at highest frequency, and this is what is observed. In Fig. 3 the results for the probe molecule NONA are also included that shows the same qualitative behavior. Within experimental accuracy, the same crossover temperature 297.5 ± 0.5 K is observed where an temperature independent spectral width is first observed on heating.

In order to further check that the change of the width of the solid-state indeed is not caused by spurious effects of the α-process we included in Fig. 3 the results of numerical simulations concerning ΔB_{285} [29] by assuming isotropic rotational diffusion, i.e., small step reorientation, for ANDRO in the limiting cases of stick and slip boundary conditions [30], taking again the relaxation time of OTP from ref. [4]. It is seen that the apparent ΔB_{285} only decreases significantly above 290 K and can not be responsible for the peculiar feature reported experimentally. In the case of large angle reorientation the effect on ΔB_{285} sets in even at higher temperatures [31].

Now we are in the position to attribute the ΔB_{ν_L} data for regimes I, II and III to a pre-averaging effect due to some motion significantly faster than the α-process and the behavior of $\Delta B_{\nu_L}(T)$ reflects that of the pre-averaged coupling constant $\overline{\delta}(T)$. Clearly, regime II and

III reveal the characteristic cusp-like temperature dependence as forecast by Eq. 1. Hence, we interpret the decrease of ΔB_{ν_L} as the decrease of $\overline{\delta}$ due to the decreasing amplitude f_{rot} of the fast dynamics which stops above $297.5K$ and thus marks the crossover temperature T_c.

We applied the approach also for the polymer PB. In Fig. 4 (top) the results of the spectral analysis at 285 GHz of TEMPO in PB are displayed. Very similar behavior is observed as in the case of OTP, and the crossover temperature is sharply marked at $T_c = 221 \pm 0.5K$. In the case of TEMPO in PB the solid-like pattern is only completely collapsed beyond 230 K again due to the influence of the α-process, however, at $f < 285$GHz the plateau region at $T > T_c$ was not any longer clearly observed.

The non-ergodicity parameter f_q (reflecting density fluctuations) of OTP and PB was measured by NS experiments [32, 33]. In Fig. 4 we included these results. It is seen that the cusp-like behavior is much less pronounced as compared to that of our EPR experiments. As already mentioned, extracting $f_q(T)$ relies on certain assumptions separating fast and slow dynamics which appear to yield the characteristics of the dynamic transition in a less defined way. In particular, vibrational contributions may hamper a clear-cut separation of the fast relaxation dynamics. In contrast the EPR analysis is based on model independent analysis of the spectra.

Conclusions - Our study shows that the reorientation of highly diluted guest molecules in both a molecular glassformer and a polymer probes a sharp anomaly which is consistent with previous less marked signatures of the IMCT transition obtained, *i.e.*, by NS experiments. We think this provides a strong case for the theory even in its ideal version. There is no masked transition. Note that the change of f_{rot} is less than 10 percent (*cf.* fig. 3) and may even be smaller in other experiments. Thus, one has to carefully re-consider previous experimental analyses in order to allow for better extracting the characteristics of the transition also in these experiments.

Acknowledgements

H.W.Spiess is warmly thanked for helpful discussions and P. Medick for carefully reading the manuscript.

* Electronic address: `dino.leporini@df.unipi.it`

[1] W. Götze, J. Phys.: Condens. Matter **11**, A1 (1999).

[2] S. P. Das, Rev. Mod. Phys. **76**, 785 (2004).

[3] W. Petry, E. Bartsch, F. Fujara, M. Kiebel, H. Sillescu, and B. Farago, Z. Phys. B **83**, 175 (1991).

[4] A.Tölle, Rep. Prog. Phys. **64**, 1473 (2001).

[5] S.V. Adichtchev et al., Phys. Rev. Lett. **88**, 055703 (2002) ; S.V. Adichtchev et al., Phys. Rev. E **68**, 011504 (2003); A. Brodin et al., Eur. Phys. J. B **44**,3 (2005).

[6] F. Mezei et al., J. Phys.: Cond. Matter **11**, A341 (1999).

[7] M. E. Cates et al, Phys. Rev. Lett. **96**, 135701 (2006).

[8] P. Mayer et al , Phys. Rev. Lett. **97**, 095702 (2006).

[9] W. van Megen, Transp. Theo. Statist. Phys. **24**, 1017 (1995); K.S.Schweizer, J.Chem.Phys. **123**, 244501 (2005).

[10] T. Franosch, W. Götze, M. R. Mayr, and A. P. Singh, Phys. Rev.E **55**, 3183, (1997).

[11] B. Ruffle', C. Ecolivet and B. Toudic, Europhys. Lett., **45**, 591 (1999).

[12] S.Wiebel and J.Wuttke, New J. Phys. **4**, 56 (2002).

[13] J. Horbach, W. Kob and K. Binder, Eur. Phys. J. B **19**, 531 (2001).

[14] C.De Michele and D.Leporini, Phys. Rev. E **63**, 036701 (2001).

[15] A. Patkowski, M. Matos Lopes, and E. W. Fischer, J.Chem.Phys. **119**, 1579 (2003).

[16] L. Andreozzi, M.Faetti, M. Giordano and D. Leporini, J.Phys.Chem.B **103** 4097 (1999) .

[17] L. Andreozzi, M.Faetti, M. Giordano and D. Leporini, J.Phys.:Condens.Matter **11**, A131 (1999).

[18] S.N. Bhat et al., Phys. Rev.Lett. **95**, 235702 (2005).

[19] K. A. Earle et al J. Chem. Phys. **106**, 9996 (1997).

[20] E. Rössler, J.Tauchert and P. Eiermann, J. Phys. Chem. **98** 8173, (1994).

[21] G. Williams and P.J. Hains, J. Chem. Soc. Faraday Symp. **6** 14 (1972).

[22] M. T. Cicerone, F. R. Blackburn and M.D.Ediger, J. Chem. Phys. **102** 471 (1995); D. Ehlich and H.Sillescu, Macromolecules, **23** 1600 (1990).

[23] T. Franosch et al., Phys. Rev. E **56**, 5659 (1997); R. Schilling, T. Scheidsteger, Phys. Rev. E **56**, 2932 (1997).

[24] J. A. Weil, J. R. Bolton, and J. E. Wertz, Electron Paramagnetic Resonance: Elementary Theory and Practical Applications (Wiley, New York, 1994).

[25] *Very High Frequency ESR /EPR*, O. Grinberg and L.J. Berliner, Eds., Biological Magnetic Resonance Vol. 22 (Kluwer, NewYork, 2004).

[26] G. Lipari, A. Szabo, J. Am. Chem. Soc. 104, 4546 (1982).

[27] G. Annino et al, Appl.Magn.Reson. **19**, 495 (2000).

[28] The definition of ΔB_{190} considers the same singularities of ΔB_{285}. The definition of ΔB_{95} takes into due account that the small doublet located at ~ 3.388 T in Fig. 2 (not present at higher frequencies) is located just in the region where the lineshape crosses the baseline at $T \sim T_c$. This limits, differently from 190 and 285 GHz, the accuracy of the location of the cross-point. We also considered the rightmost peak of the lineshape at 95 GHz to get better accuracy at higher temperatures.

[29] M.Giordano, P.Grigolini, D.Leporini, P.Marin, Phys.Rev.A **28**, 2474 (1983).

[30] B.J. Berne, R.Pecora, Dynamic Light Scattering (Dover, New York 2000).

[31] V.Bercu, M.Martinelli, C.A. Massa, L.A. Pardi, D.Leporini, J.Chem.Phys. **123** 174906 (2005).

[32] A. Tölle et al., Phys. Rev. E **56**, 809 (1997).

[33] B. Frick et al., Phys. Rev. Lett. **64**, 2921 (1990).

FIG. 1: Temperature dependence of the HF-EPR lineshape at $\nu_L = 285$ GHz of ANDRO in OTP ($cf.$ fig. 3). Top: overview. The corresponding structural relaxation times and the equivalent frequency shift are also indicated. Bottom: detailed view in the range $292.1K \leq T \leq 307.3K$.

FIG. 2: HF-EPR lineshape of ANDRO in OTP at $\nu_L = 95GHz$, $281.2K$ (left) and $\nu_L = 285GHz$, $276.3K$ (right). See text for details.

FIG. 3: Temperature dependence of ΔB_{ν_L} of the spin probe ANDRO ($\nu_L = 95, 190, 285$) GHz and NONA ($\nu_L = 285$ GHz) in OTP. Stars denote points concerning ΔB_{250} from ref. [19]. All curves (but the one denoted by red dots) are shifted vertically to make the comparison easier. Black curves are theoretical simulations [29] of ΔB_{285} approximating ANDRO to a prolate ellipsoid diffusing due to the α-process with either stick (continuous) or slip (dashed) boundary conditions.

FIG. 4: Comparison between HF-EPR results and neutron scattering data for OTP [32] and PB [33]. Top: ΔB_{285} of TEMPO in PB. Bottom: ΔB_{285} of ANDRO in OTP.

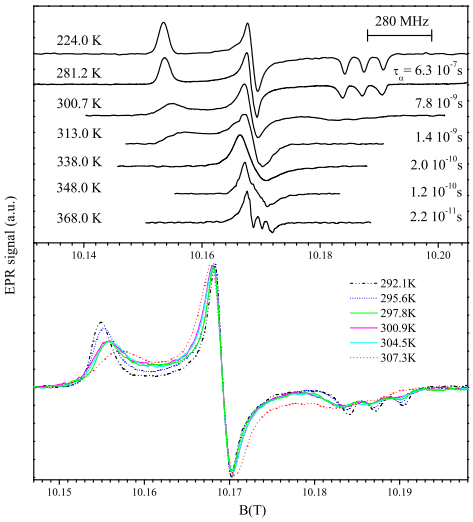
280 MHz
224.0 K
281.2 K
300.7 K
313.0 K
338.0 K
348.0 K
368.0 K
τα = 6.3 10-7s
7.8 10-8s
1.4 10-9s
2.0 10-10s
1.2 10-10s
2.2 10-11s
10.14
10.16
10.18
10.20
292.1K
295.6K
297.8K
300.9K
304.5K
307.3K
EPR signal (a.u.)
10.15
10.16
10.17
10.18
10.19
B(T)

FIGURE 1

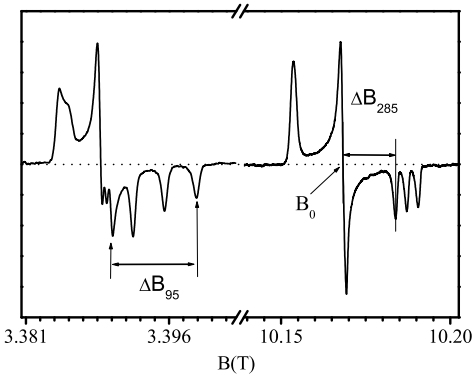

FIGURE 2

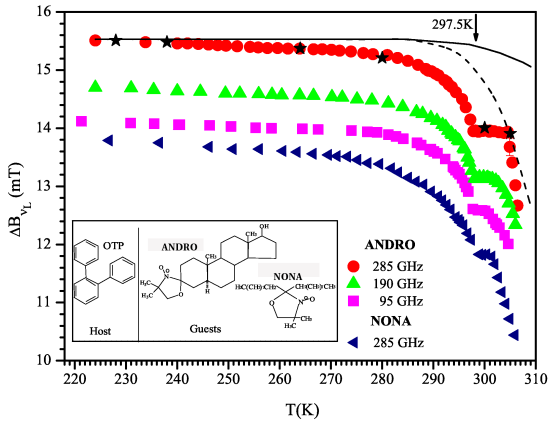
297.5K
ΔB_vL (mT)
T(K)
OTP
ANDRO
NONA
Host
Guests
ANDRO
285 GHz
190 GHz
95 GHz
NONA
285 GHz

FIGURE 3

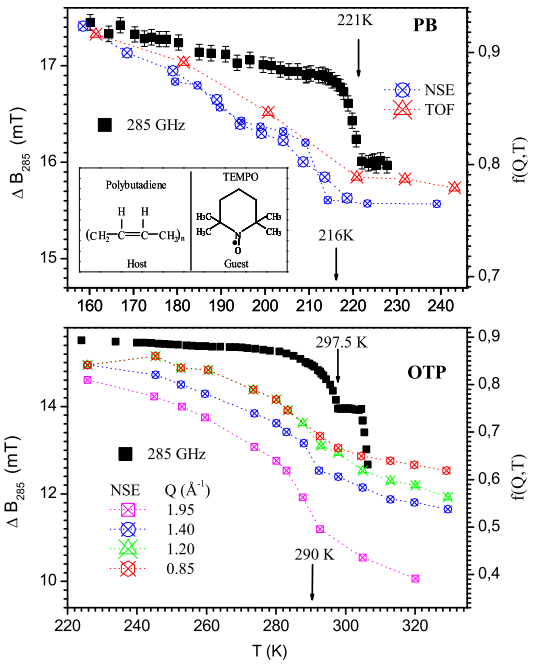
221K
PB
NSE
TOF
285 GHz
Polybutadiene
TEMPO
Host
Guest
216K
297.5 K
OTP
285 GHz
NSE Q (Å⁻¹)
1.95
1.40
1.20
0.85
290 K
Δ B285 (mT)
f(Q,T)
T (K)

FIGURE 4